Optimal design and operation of a waste tire feedstock polygeneration system

Avinash S.R. Subramanian[a], Truls Gundersen[a], Thomas A. Adams II[b]

[a]*Department of Energy and Process Engineering, Norwegian University of Science and Technology (NTNU), Kolbjørn Hejes vei 1B, NO-7491, Trondheim, Norway.*
[b]*Department of Chemical Engineering, McMaster University, 1280 Main St. W, Hamilton, ON, Canada, L8S 4L7.*

Abstract

The optimal design and operation of a polygeneration system that uses a waste tire feedstock to produce a mix of electricity, fuels and chemicals is presented. Rigorous mass and energy balance models for the process are developed from which data are generated to fit surrogate models. The optimization problem is formulated as a nonconvex Mixed-Integer Nonlinear Program (MINLP) and solved to global optimality using ANTIGONE. The influence of variation in product prices and carbon dioxide (CO_2) tax rates on the optimal process design and operation is also presented. In all scenarios studied, the optimal product portfolio favors generation of one fuel or chemical together with electricity. Electricity generation is favored in a base case with historically average market prices, while methanol, liquefied Synthetic Natural Gas (SNG) and Dimethyl Ether (DME) are favored in relatively probable scenarios in which the corresponding product fetches higher prices. Pre-combustion CO_2 capture is favored at lower CO_2 tax rates while post-combustion CO_2 capture is only optimal in scenarios with higher rates. The optimal product portfolio changes substantially with varying market conditions thus motivating future work on designing flexible polygeneration processes that have the capacity to adjust operating conditions in order to maximize profitability by exploiting price peaks.

Keywords: Polygeneration system, Waste-to-Energy, Gasification, Global optimization, CO_2 capture, Waste Tire, Rubber

1. Introduction

Polygeneration systems produce multiple products, typically a mix of electricity, fuels (gasoline, diesel, SNG, hydrogen) and chemicals (methanol, DME, olefins, acetic acid), and as such offer several economic and environmental advantages over single product systems. Research interest in polygeneration has been motivated partly by the fact that these processes have a greater ability to maintain profitability in the face of significant market uncertainties as a result of the diverse product portfolio. Polygeneration plants that utilize alternative feedstocks such as solid wastes (waste tires, plastics and municipal solid waste) and implement a CO_2 capture technology may also fit into an environmentally conscious business strategy. A review of polygeneration is presented by Adams and Ghouse [1].

The use of wastes is particularly important because increased population growth is expected to create even larger waste quantities that require appropriate management. For instance, in the developed world, approximately 1 waste tire per person per year is produced resulting in approximately 1 billion discarded tires annually [2]. In addition, there are currently an estimated 4 billion waste tires in landfills and stockpiles worldwide highlighting the extent of the disposal problem. Waste tires are a particularly suitable feedstock for conversion to high-value products through gasification as a result of their homogeneous nature, high energy density (Lower Heating Value (LHV) of $\sim$33.96 MJ/kg, higher than coal), high volatile matter content ($\sim$67%) and low ash content ($\sim$7%).

In a previous work, we investigated steam gasification of waste tire in a rotary kiln to produce liquefied SNG [3]. While rotary kiln gasifiers have certain advantages, they may not be suitable for large scale systems because of the need for expensive syngas compression and tar cracking processes. Entrained flow (EF) gasification, with essentially the same gasifier design used commercially for coal gasification, is a highly efficient, high temperature process that has the substantial advantage of complete tar cracking and removal [4]. Although EF gasification has certain drawbacks (such as higher cost, tight restriction on feedstock quality, requirement of additional units for feedstock and slurry preparation [5]), Larson et al. [4] and Boerrigter and van der Drift [6] suggest that EF gasification is the most suitable option at least for large scale biomass conversion, thus this option is used in this work. We note however that it is technically feasible to use other gasifier types that operate at lower temperatures or pressures.

Several research efforts have studied polygeneration processes that utilize at least one alternative feedstock. Chen et al. studied the global optimal design and operation of a process in which coal and biomass are co-gasified in an EF gasifier to produce a mix of naphtha, diesel, methanol and electricity using both a deterministic model [7] and a stochastic model that takes uncertainty into account [8]. The results showed that the proportion of biomass feedstock utilized depended strongly on carbon tax and the biomass price. Baliban et al. studied the optimal design of a biomass, coal and natural gas to gasoline, kerosene and diesel process [9] using both local and global optimization algorithms ([10] extended in [11]). Niziolek et al. studied the conversion of municipal solid waste to methanol, gasoline or olefins with the results suggesting that levying tipping fees enabled the process to become cost-competitive with fossil-fuel based alternatives [12]. Salkuyeh and Adams studied the optimal design of a petcoke and natural gas based process for polygeneration of methanol, DME, olefins and electricity using a particle swarm optimization strategy linked to rigorous Aspen Plus models [13]. This work was extended by Salkuyeh et al. where biomass was considered as an additional feedstock and ethanol and Fischer-Tropsch liquids were considered as additional products [14], with the results suggesting that profitability could be achieved with feedstock mixes containing up to 65% petcoke/biomass.

Although these studies highlight the promise of alternative fuels generally, further research is necessary to analyze the use of waste rubber tires especially from the systems perspective at industrially relevant scales. In addition, to the best of the authors' knowledge, no studies have been performed on the detailed process simulation and techno-economic optimization of waste tire conversion systems using EF gasifiers. Therefore the objective of this paper is to investigate the optimal design and operation of a polygeneration system that converts a waste tire feedstock to a mix of electricity, methanol, DME, olefins and liquefied SNG. Rigorous process models in Aspen Plus and Aspen HYSYS are developed from which sample data are generated to fit surrogate models using the ALAMO software (presented in [15] using the approach discussed in [16]). The optimization problem is formulated as a MINLP and solved to global optimality using ANTIGONE [17]. The influence of variation in the prices of the different products and CO_2 taxes on the optimal process design and operation is also presented.

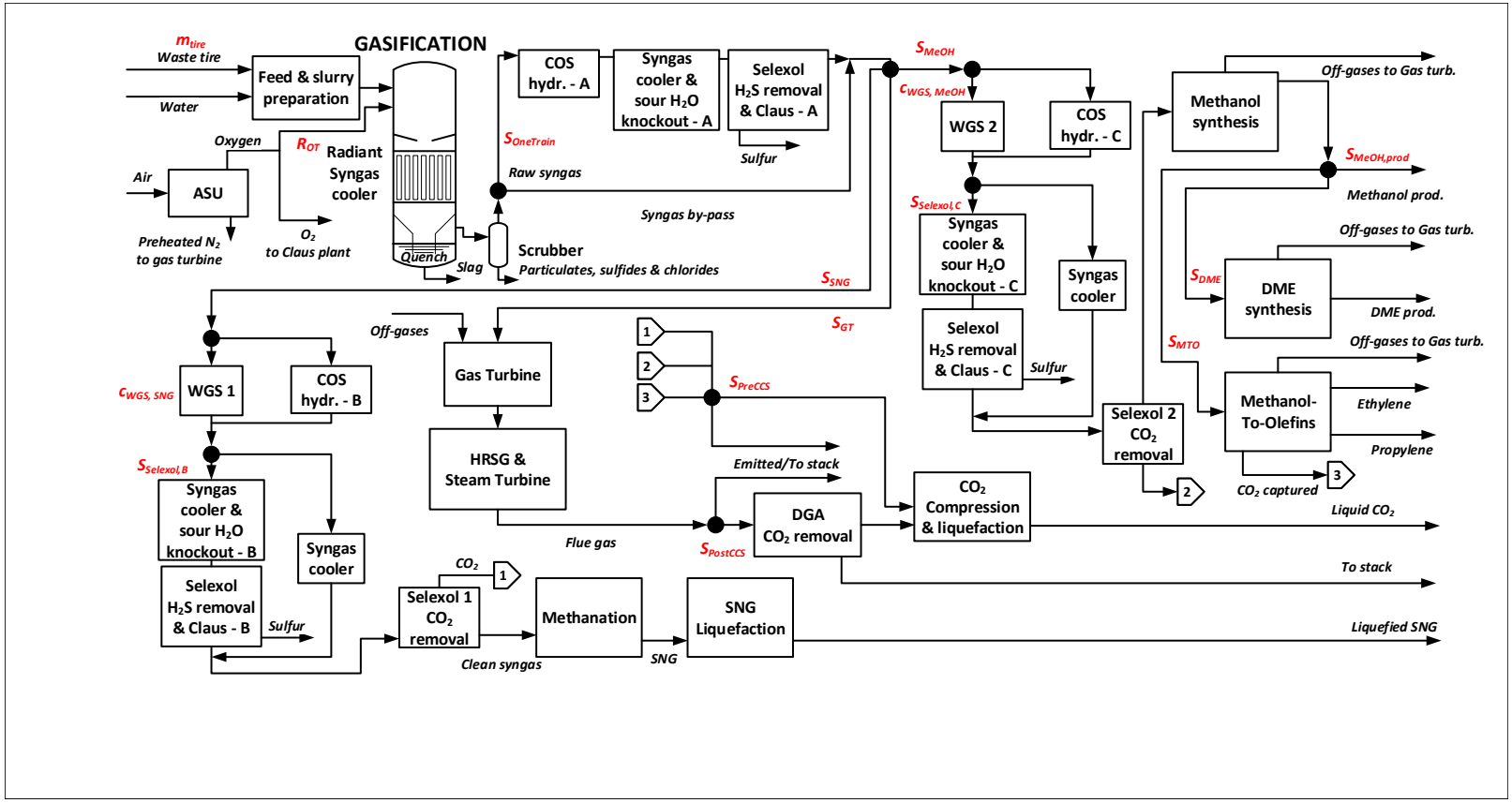

Figure 1: Superstructure of the solid waste tire feedstock polygeneration system

Unit	Parameters	Reference
Feedstock	Ultimate (wt%): C: 77.3, H: 6.2, N: 0.6, S: 1.8, O: 7.3, Ash: 6.8	[3]
	Proximate (wt%): Volatile Matter (VM): 67.7, Fixed Carbon (FC): 25.5, Ash: 6.8	
Air Separation Unit (ASU)	Oxygen purity: 99.5 mol%, Recovery pressure P = 10 bar	[18], [19]
Waste tire preparation	Crumb size = 0.18 mm	[20]
Gasification	EF gasification. 29.11 wt% water/70.88wt% waste tire, P = 56 bar	[21]
	Ash melting energy: (1.0 kJ/kg_{ash})	[22]
Water Gas Shift (WGS)	High temperature WGS: T = 420 °C, P = 54 bar	[23], [18]
Carbonyl Sulfide (COS) hydrolysis	T = 200 °C, P = 54 bar	
Hydrogen Sulfide (H_2S) removal	Solvent composition: 62.3 mol% Dimethyl Ether of Polythene Glycol (DEPG): 37.7 mol% H_2O	[24]
	T = 40 °C, 53.5 bar, Removal: 92.7 mol% H_2S	
CO_2 removal	Solvent composition: 63.9 mol% DEPG: 36.1 mol% H_2O	[24]
	T = 20 °C, P = 53.5 bar, Removal: 96.9 mol% CO_2	
Claus process	Two-stage sulfur conversion, Furnace: T = 950 °C	[25]
Methanation	Four-stage conversion, Inlet T = 300 °C, Inlet P = 53.6 bar.	[26]
	Adiabatic reactors. Total ΔP = 3 bar (across 4 stages), Recycle ratio = 75 %	
SNG compression & purification	Outlet pressure = 55 bar	[25], [3]
SNG liquefaction	SNG flow rate = 9.7 kg/s, P = 55 bar, Inlet T = 22 °C, Outlet T = -157 °C	[27]
	Multistream Heat Exchanger (MSHE) UA_{max} = 25.0 MW/K, Pressure ratio = 6.5	
	Refrigerant mole composition: N_2: 8.3, CH_4: 24.0, C_2H_6: 36.9, n-C_4H_{10}: 30.8	
	Low P = 2.8 bar, high P = 18.0 bar, ΔT_{min} = 0.95 K, Flow rate = 58.5 kg/s	
Methanol synthesis & purification	T = 240 °C, P = 51 bar, Recycle ratio = 85 % , Off-gases to GT,Purity: 99.5 mol%	[28], [29]
DME synthesis & purification	T = 280 °C, P = 50 bar, Off-gases to GT	[29], [30]
	DME Purification column, Purity: 99.5 mol%	
Methanol-To-Olefins (MTO) & purification	T = 400 °C, P = 40 bar, Off-gases to GT	[31]
	CO_2 absorption unit. Absorbent: 70.0 wt% Diglycol Amine (DGA): 30.0 wt% H_2O, Absorber: 2 bar, Regenerator: 1.5 bar, Purity 99.9 mol%	
	De-ethanizer, 35 bar Ethane recovery: 99.80 %, Power consumption: 0.35 MWe/$MW_{LHV,Ethane}$	
	De-methanizer, 34 bar Methane removal: 99.99 % Power consumption: 1.21 MWe/$MW_{LHV,Methane}$	
	C2-splitter, 10 bar, Ethylene recovery: 95.00 %, purity: 99.9 mol%, Power consumption: 0.64 MWe/$MW_{LHV,Ethylene}$	
	De-propanizer, 25 bar, Propylene recovery: 98.00 %, purity: 99.2 mol%	
Gas Turbine	Thermal Efficiency: 46.8 % (Ratio of Net Power out [MW] to Total LHV of input fuel)	Simulation
Steam Turbine	Thermal Efficiency (High Quality heat): 44.1 %, Thermal Efficiency (Low Quality heat): 15.4 % (Details in Supp. Mat.)	[32], [7]
Postcombustion CO_2 capture	Solvent composition: 72.3 wt% DGA: 27.3 wt% H_2O	[24], [3]
	T = 70 °C, P = 1.0 bar, CO_2 Removal = 95.0 mol%	
CO_2 compression	Multistage compressors, CO_2 purity = 99.1 mol%, Outlet T = 25 °C, P = 153 bar	[19]
CO_2 transportation and sequestration	Operating cost: 12.5 $/tonne	[23]
Compressors	Isentropic efficiency = 80 %, maximum pressure ratio = 5	[23]
Pumps	Efficiency = 80 %	[23]

Table 1: Operating parameters and specifications

2. Process Simulation and generation of Surrogate Models

Figure 1 presents a superstructure of the polygeneration concept that converts a waste tire feedstock to several possible products including methanol, DME, olefins, liquefied SNG or electricity.

The key decision variables for the optimal design and operation problem are presented in Figure 1 (in red) and described in Table 2. The tire feedstock mass flow rate is denoted by m_{tire}, which is the only extensive decision variable of the optimization problem. The variable m_{tire} also determines the overall plant scale measured by total thermal input which is constrained to be less than 893 MW_{LHV} in order to be consistent with previous studies [3], [4]. Based on data presented in [20], we calculate that this corresponds to a maximum requirement of approximately 82.7 million tires per year which is only $\sim$ 2 % of the amount of waste tires existing in stockpiles worldwide or $\sim$ 8 % of the amount discarded in the developed world every year. While we note that there are certain logistical challenges to collecting such large waste tire quantities in one location, the objective of this work is to evaluate if such a concept is economically feasible. We also note that there already exist several large scale waste tire collection efforts worldwide. In addition, all the technical results and calculations scale linearly with the total thermal input thus allowing the consideration of smaller scale projects.

The ratio of the oxygen to the tire mass flow rate (R_{OT}) is a decision variable that determines both the total gasifier input flow rate and the gasification temperature, and thus the raw syngas composition. Generally, gasification at lower R_{OT} ratios produces syngas with higher H_2/CO ratios at the expense of lower yields.

After passing through a scrubber, the raw syngas either heads to a "one train" sulfur removal system consisting of a COS hydrolysis reactor, syngas cooler & sour H_2O knockout drum and a Selexol-based H_2S removal unit & Claus plant or bypasses this system. A binary decision variable $S_{OneTrain}$ is implemented to represent this choice. The split fraction of syngas sent to the methanation, methanol synthesis and gas turbine sections is given by S_{SNG}, S_{MeOH} and S_{GT} respectively. Prior to methanation or methanol synthesis, the syngas can be upgraded using a WGS reaction; the respective conversions of CO ($c_{WGS,SNG}$ and $c_{WGS,MeOH}$) are decision variables. High conversion results in hydrogen-rich syngas at the expense of higher steam consumption and lower energy efficiency. COS hydrolysis occurs simultaneously in the WGS reactors.

In the methanation and methanol synthesis trains, binary variables $S_{Selexol,B}$ and $S_{Selexol,C}$ are implemented to denote the choice of directing the corresponding syngas streams to sulfur removal systems B or C respectively. Constraints on the allowable mole fractions of COS and H_2S are imposed on the streams heading to the methanation, gas turbine and methanol synthesis sections. The motivation for devising this superstructure is as follows: If multiple products trains are favored simultaneously, it is expected that the optimal configuration would implement the one train sulfur removal system in order to avoid building multiple downstream selexol H_2S removal units. However, if either the methanation or methanol synthesis trains are favored individually (together with a WGS unit), it is expected that the optimal configuration involves bypassing the one train sulfur removal system and instead implementing the corresponding Selexol B or C H_2S removal units (since these two trains do not require a COS hydrolysis section). If only the gas turbine train is favored, then the constraints on H_2S and COS would require the implementation of the one train sulfur removal system.

The methanol produced could be further processed to DME, olefins or sold as final product with the corresponding split fractions given by S_{DME}, S_{MTO} and $S_{MeOH,prod}$. The split fraction of flue gas sent to the DGA-based postcombustion carbon capture and sequestration (CCS) process is denoted by $S_{PostCCS}$. The fraction of the CO_2 captured in the Selexol and MTO section that is sent to the CO_2 compression, liquefaction and sequestration section is given by S_{PreCCS}.

Mass and energy balances are first implemented using rigorous models in Aspen Plus v10 for most unit operations except for the Selexol-based H_2S and CO_2 removal sections which are modeled using Aspen HYSYS v10. The Peng-Robinson equation of state with the Boston-Mathias modification (PR-BM) was used for physical property calculations for most units (consistent with previous work [23] followed in [3]) except the methanation section (for which the Redlich-Kwong-Soave equation of state with modified Huron-Vidal mixing rules (RKS-VM) was used as validated in [33]), the Selexol-based H_2S and CO_2 removal sections (for which the DBR amines package was used) and the DGA-based CO_2 removal section (for which the ElecNRTL package was used). Table 1 presents a summary of the operating parameters and assumptions for the process simulation.

These rigorous process simulations were then used to generate sample data points for fitting surrogate mass and energy balance models for the unit operations in order to keep the optimization problem tractable for global

optimization solvers. The ALAMO software was used for generating the surrogate models which were in the form of algebraic functions relating the state variables of the unit operation (such as mass, heat and work flow rates) to relevant decision variables listed in Table 2 [15]. In order to reduce the number of independent decision variables (and thus the dimensionality of the surrogate models), certain auxiliary variables were introduced as suggested by Straus and Skogestad ([34] extended further in [35]). For instance for a reactor, extents of each reaction were introduced. Thus, the surrogate model takes the form of an algebraic function relating the reaction extents to relevant decision variables (an example for the gasifier is given by Equation 2). An additional equation enforcing species mass balance constraints for the reactor (Equation 1) is also implemented (where $f_{in,i}$ and $f_{out,i}$ are the molar flow rates of component i entering and leaving the reactor respectively, ξ_r is the extent of reaction r, $\nu_{i,r}$ is the stoichiometric coefficient of component i in reaction r, and N_{rxns} is the total number of reactions occurring). Polynomial (up to order 4), exponential, logarithmic and constant basis functions are considered for the surrogate models. The Bayesian Information Criterion (BIC) was used in ALAMO as a model fitness metric to balance the bias-variance trade-offs as suggested by Wilson and Sahinidis [15]. The following sections present an overview of key process units; the complete model is presented in the Supplementary Material. The modeling file is made open-source at the LAPSE digital archive at:
http://psecommunity.org/LAPSE:2020.1034 [36].

$$f_{out,i} = f_{in,i} + \sum_{r=1}^{N_{rxns}} \nu_{i,r}\xi_r \tag{1}$$

2.1. Air Separation Unit

Oxygen of high purity (99.5 mol%) is produced using a cryogenic ASU and compressed for use in the gasification and Claus processes. The modeling approach detailed in [18] is used.

2.2. Tire Feedstock and Slurry preparation

Waste tires received at the plant gate are shredded and ground to a maximum size of 0.18 mm as required for EF gasification [21]. The parasitic electricity load for grinding is estimated based on correlations presented in [20] as described in [3]. The tire feedstock is then mixed with water to form a slurry (29.11 wt% water/70.88 wt% tire) that is fed to the gasifier.

2.3. Entrained flow gasification

The tire slurry together with oxygen from the ASU is fed to a downdraft EF gasifier [23]. The gasification phenomena include pyrolysis, devolatilization, char gasification, sulfur reaction, and a complex series of chemical reactions to give a gaseous product (consisting primarily of H_2, CO and CO_2). The syngas generated is assumed to be tar-free since complete tar cracking typically occurs in EF gasifiers [4]. The hot syngas flows downwards and is cooled in a radiant syngas cooler (RSC) to 677 °C and then passes through a water quench and syngas scrubbing system for removal of particulates, sulfides and chlorides [21]. Non-combustible tire components flow down the walls of the gasifier and exit as slag [23].

The EF gasifier is modeled using the approach suggested by Kunze and Spliethoff [22] and followed in [23]: The pyrolysis (breakdown) of the solid char to reactive compounds is first modeled as a decomposition process in an RYIELD block together with a calculator block to specify the component yields according to the ultimate composition of tire (details in the Supplementary Material). Following this, the gasification reactions are modeled using an RGIBBS reactor assuming chemical equilibrium conditions. A heat loss to the environment of 1% of the LHV of waste tire is assumed. The following six reactions occur:

$$\mathrm{C} + \mathrm{O_2} \rightleftharpoons \mathrm{CO_2} \tag{GR1}$$

$$\mathrm{C} + \mathrm{CO_2} \rightleftharpoons 2\,\mathrm{CO} \tag{GR2}$$

$$\mathrm{CO} + 3\,\mathrm{H_2} \rightleftharpoons \mathrm{CH_4} + \mathrm{H_2O} \tag{GR3}$$

$$\mathrm{CO} + \mathrm{H_2O} \rightleftharpoons \mathrm{H_2} + \mathrm{CO_2} \tag{GR4}$$

$$\mathrm{H_2} + \mathrm{S} \rightleftharpoons \mathrm{H_2S} \tag{GR5}$$

$$\mathrm{CO} + \mathrm{S} \rightleftharpoons \mathrm{COS} \tag{GR6}$$

Surrogate models for the gasifier are developed using data generated from the Aspen Plus model (RYIELD, RGIBBS and RSC). In particular, the surrogate model for the extent ($\xi_{gr,EF}$) of each reaction gr is presented in

Equation 2 highlighting the nonlinear dependence on the relevant intensive decision variable (R_{OT}) and the linear dependence on the extensive variable (m_{tire}). Species mass balance in the gasifier is enforced by an additional constraint of the form of Equation 1. Similarly, the heat rejected by the gasifier is given by Equation 3, where $Q_{HQ,EF}$ is the duty of the RSC (in MW). The values of the coefficients are presented in the Supplementary Material.

$$\begin{aligned}\xi_{gr,EF} = m_{tire}.(&\beta_{0,EF,gr} + \beta_{1,EF,gr}.R_{OT} + \beta_{2,EF,gr}.R_{OT}^2 + \beta_{3,EF,gr}.R_{OT}^3 \\ &+ \beta_{4,EF,gr}.R_{OT}^4 + \beta_{5,EF,gr}.exp(R_{OT}) + \beta_{6,EF,gr}.log(R_{OT})), \\ &\forall gr \in \{\text{GR1, GR2, ... , GR6}\}\end{aligned} \tag{2}$$

$$\begin{aligned}Q_{HQ,EF} = m_{tire}.(&\beta_{0,EF,Q} + \beta_{1,EF,Q}.R_{OT} + \beta_{2,EF,Q}.R_{OT}^2 + \beta_{3,EF,Q}.R_{OT}^3 \\ &+ \beta_{4,EF,Q}.R_{OT}^4 + \beta_{5,EF,Q}.exp(R_{OT}) + \beta_{6,EF,Q}.log(R_{OT}))\end{aligned} \tag{3}$$

2.4. Sulfur removal sections

Prior to sulfur removal, any COS in the syngas streams needs to be converted to H_2S either in a dedicated COS hydrolysis reactor (A, B or C) or concurrently in a WGS reactor (1 or 2) [23]. The syngas is then cooled and the sour water knocked out and treated. The syngas stream then enters a Selexol-based H_2S removal section (A, B or C) in which H_2S is removed. The H_2S rich stream from the stripping section heads to Claus plants for conversion into elemental sulfur as a valuable by-product. The modeling approach detailed in [37] is used. Constraints on the allowable mole fractions of COS and H_2S are imposed prior to downstream synthesis.

2.5. Water Gas Shift

Syngas destined for the methanation or methanol synthesis section can be upgraded by diverting a portion of the stream to a WGS reactor as explained in [23]. High-temperature WGS is implemented in order to allow an overall conversion of up to 80%. Since the overall conversions ($c_{WGS,SNG}$ or $c_{WGS,MeOH}$) can be adjusted by varying the split fractions to the WGS reactors, we formulate the surrogate mass balance model by considering $c_{WGS,SNG}$ (or $c_{WGS,MeOH}$) as the relevant intensive decision variables similar to the approach in [7]. Thus, for the SNG train, overall extent of reaction ($\xi_{WGS,METH}$)

can be calculated using Equation 4, and an additional constraint in the form of Equation 1 is implemented.

$$\xi_{WGS,METH} = \frac{f_{WGS1\_feed,\mathrm{CO}} \cdot c_{WGS,SNG}}{\nu_{CO,WGS}} \tag{4}$$

2.6. CO_2 removal

A selexol-based process CO_2 removal is implemented for the methanation and methanol synthesis trains ([23]). The parasitic work and heat loads for the H_2S and CO_2 removal sections are given as functions of the molar flowrates of H_2S and CO_2 in the respective feed streams.

2.7. Methanation and SNG Liquefaction

The TREMP methanation process was used with a model similar to previous work [3] and Ref. [26]. The syngas composition heading to the methanation process is constrained such that the "feed gas module" M (given by Equation 5), that accounts for the presence of CO_2 in the syngas feed, is set to 3 to maximize methane production [38]. The feed syngas composition as well as all methanation operating conditions are fixed, thus the overall conversion is constant. For this reason, the production rate of methane is implemented as a linear function of the input flow rate. The SNG product stream is passed through a molecular sieve in order to remove any remaining water to sub-ppm levels and 98.5 vol% of CO_2. Molecular sieves are designed to separate molecules based on differences in polarity and molecular size as detailed in Ref. [39]. The SNG stream is then compressed to 55 bar in order to satisfy specifications of liquefaction [25].

$$M = \frac{f_{METH\_in,\mathrm{H_2},} - f_{METH\_in,\mathrm{CO_2}}}{f_{METH\_in,\mathrm{CO}} + f_{METH\_in,\mathrm{CO_2}}} = 3.0 \tag{5}$$

The Single Mixed Refrigerant process is implemented for SNG liquefaction. Thus the pressurized SNG stream is desuperheated, liquefied, and subcooled in a multistream plate-and-fin type heat exchanger before exiting as liquefied SNG at -157 °C with the cooling duty provided by a single refrigeration cycle. The process is simulated using the approach detailed in our previous work [3] and in Ref. [27]. The SNG flow rate remains unchanged, thus mass balance holds trivially, and the parasitic work and heat requirements are expressed as linear functions of the input SNG mass flowrate.

2.8. Methanol synthesis

A kinetic model for the hydrogenation of CO and CO_2 to methanol is implemented according to the approach suggested in [40] and followed in [29]. In order to maximize the production of methanol, the feed syngas composition (before recycle) is constrained such that the H_2/CO ratio is 2.0. A portion of the unreacted syngas is also recycled. By-products consisting of higher alcohols and off-gases are sent to the gas turbine for combustion and additional electricity generation [23]. The feed syngas composition as well as all operating conditions are fixed, thus the overall conversion is constant. This implies that the production rate of methanol has only a linear dependence on the input syngas flow rate. The produced methanol product could be further processed to DME, olefins or sold as final product.

2.8.1. DME synthesis

A kinetic model for the dehydration of methanol to DME is implemented using the approach detailed in [41] and followed in [29]. The operating conditions are fixed thus the product flow rate is a linear function of the feed flowrate.

2.8.2. Methanol to Olefins (MTO)

The dehydration of methanol to produce ethylene, propylene and other hydrocarbons is modeled using the approach suggested in [31]. The product is first sent to a DGA-based CO_2 absorber before heading to a de-ethanizer column to remove ethylene, ethane and other light gases from the propylene and heavier components. The lighter stream heads to a de-methanizer and finally a C2-splitter to yield pure ethylene with the rest of the off-gases sent to the gas turbine. The heavier components are sent to a de-propanizer to yield propylene with the off-gases sent to the gas turbine. The de-methanizer and C2-splitter are sub-ambient temperature processes thus refrigeration is required with the work requirement estimated from data provided in [31]. As before, the operating conditions are fixed thus the product flow rates exhibit a linear dependence on the feed flow rate.

2.9. Gas Turbine

The third syngas branch together with off-gases from methanol synthesis, DME synthesis and MTO processes head to a gas turbine. The electricity generated (W_{GT}) is calculated using Equation 6 where $Q_{GT,in}$ is the total

thermal input (on a LHV basis); the gas turbine efficiency (η_{GT}) is specified in the Supplementary Material.

$$W_{GT} = \eta_{GT}.Q_{GT,in} \tag{6}$$

2.10. Steam Generation and Steam Turbine system

Net surplus heat from the above process units is converted to steam which is used to generate electricity in a steam turbine. Following the approach in [7], a division into high quality (HQ) and low quality (LQ) heat is used together with corresponding steam turbine efficiency values ($\eta_{ST,HQ}$ and $\eta_{ST,LQ}$). The work generated in the steam turbine (W_{ST}) is given by Equation 7, where the net HQ and LQ heat available is denoted by Q_{HQ_net} and Q_{LQ_net} respectively. The net work generated in the process (W_{net}) is given by Equation 8 where $W_{parasitic}$ denotes the overall parasitic electricity load.

$$W_{ST} = \eta_{ST,HQ}.Q_{HQ\_net} + \eta_{ST,LQ}.Q_{LQ\_net} \tag{7}$$

$$W_{net} = W_{ST} + W_{GT} - W_{parasitic} \tag{8}$$

2.11. DGA-based postcombustion CO_2 capture

Flue gas exiting the Heat Recovery Steam Generator (HRSG) is either emitted or heads to the DGA section for postcombustion CO_2 capture. This process is similar to the Selexol unit and is modeled with the approach detailed in our previous work [3]. The parasitic work and heat load scales linearly with the mass flow rate of CO_2 in the flue gas stream. The captured CO_2 together with the CO_2-rich streams from the Selexol section and the MTO section is compressed, liquefied and injected into a pipeline destined for sequestration. The work, heat and operating cost is modeled assuming linear dependence on mass flow rate.

3. Optimization Problem formulation

The optimal design and operation problem is formulated as a nonconvex Mixed-Integer Nonlinear Program (Equation 9) where Net Present Value (NPV) is used as the objective function. A discrete set of possible equipment sizes were considered for each process section and binary variables ($\mathbf{y}$) were

used to represent the choice of picking a particular size as detailed in [42]. Thus, the objective function exhibited a linear dependence on these binary variables. We note that we also implemented a nonconvex Nonlinear Program (NLP) formulation, with a concave objective function to denote the economy of scale relations and using only continuous decision variables, but in all cases the solution time exceeded our maximum limit of 10,000 s. NPV is calculated using the discounted cash flow rate of return approach [43] with the assumptions made by Chen et al. [7]. The total capital cost (Cap) of the different pieces of equipment are estimated based on data from literature. Pro_{net} denotes the annual net profit. The product prices, CO_2 tax rates and waste tire tipping fees used for the 7 cases as well as the sources used to obtain this data are presented in Table 3. Case 1 represents a scenario with historically average market conditions while Cases 2 - 5 represent scenarios in which one of the products fetches an unusually high price as indicated in the Table. Case 6 represents a scenario when CO_2 taxes of 100 \$/tonne are implemented while Case 7 denotes a scenario when waste tire tipping fees of 100 \$/tonne are levied.

Fixed operating costs (labor, maintenance, operating overhead, and property insurance & tax costs) as well as variable operating costs (electricity and utilities, raw material, catalyst and solvent, waste disposal costs) are estimated from literature sources such as references [43] and [21]. Parameters for the tax rate (R_{tax}), annual discount rate (r), depreciation time (t_{dp}), project lifetime (t_{lf}) as well as data used for economic modeling are presented in the Supplementary Material. An availability factor of 85% is assumed for all units of the process. Thus, we assume that the plant operates 85% of the time (equivalent to 7446 hours in a year). All costs are scaled to US$\$_{2018}$ assuming a yearly inflation rate of 2.75%.

The decision variables $\mathbf{x}$ are listed in Table 2. The optimization problem is formulated using the recently developed GOSSIP software [44] and solved to global optimality using ANTIGONE [17]. The resulting MINLP problem has 270 binary variables for the design decisions $\mathbf{y}$ (as 27 process sections are implemented with 10 discrete section sizes available), 930 continuous and 5 binary operational variables. There are 27 equality constraints involving the binary $\mathbf{y}$ variables, and 937 constraints (903 equality and 34 inequality) involving the continuous variables. Nonconvexities arise due to bilinear terms in the mass balance model, the gasifier surrogate model (which is a set of highly nonlinear equality constraints) and the discrete choice of equipment sizes.

$$\begin{aligned} \max_{\mathbf{y},\,\mathbf{x}} \quad & \text{NPV} = Cap(\mathbf{y})\Big[-1+\frac{R_{tax}}{r.t_{dp}}\Big(1-\frac{1}{(1+r)^{t_{dp}}}\Big)\Big] + Pro_{net}(\mathbf{x})\Big[\frac{1}{r}\Big(1-\frac{1}{(1+r)^{t_{lf}}}\Big)\Big] \\ \text{s.t.} \quad & \text{Mass and energy balances, Operating cost model, Capital cost model} \\ & \text{Scale constraints} \end{aligned} \tag{9}$$

Decision Variable	Description	Units	LBD	UBD
m_{tire}	Mass flow rate of waste tire fed to gasifier	kg/s	0.0	30.0
R_{OT}	Ratio of pure oxygen to tire mass flow rate fed to gasifier		0.25	1.25
$S_{OneTrain}$	Binary choice of one train [1] sulfur removal system		0	1
$c_{WGS,SNG}$	Overall conversion of CO in the WGS reactors prior to methanation		0.0	0.8
$c_{WGS,MeOH}$	Overall conversion of CO in the WGS reactors prior to methanol synthesis		0.0	0.8
S_{SNG}	Split fraction of clean syngas sent to the methanation section		0.0	1.0
S_{MeOH}	Split fraction of the clean syngas sent to the methanol synthesis section		0.0	1.0
S_{GT}	Split fraction of the clean syngas sent to the gas turbine section		0.0	1.0
$S_{Selexol,B}$	Binary choice of sulfur removal implemented in the methanation train		0	1
$S_{Selexol,C}$	Binary choice of sulfur removal implemented in the methanol synthesis train		0	1
$S_{MeOH,prod}$	Split fraction of methanol sold as product		0.0	1.0
S_{DME}	Split fraction of methanol product sent to the DME synthesis section		0.0	1.0
S_{MTO}	Split fraction of methanol product sent to MTO synthesis section		0.0	1.0
$S_{PostCCS}$	Split fraction of flue gas sent to the DGA-based postcombustion CCS section		0.0	1.0
S_{PreCCS}	Split fraction of CO_2 removed in other plant sections[2] sent to sequestration		0.0	1.0

Table 2: Key decision variables of the optimization problem. [1] The one train sulfur removal system is implemented prior to the syngas stream split to downstream synthesis sections. [2] This includes CO_2 removed in the Selexol sections and in the MTO section prior to the De-ethanizer

Parameter	Description	Units	Case 1 Historical	Case 2 $\uparrow P_{NG}$	Case 3 $\uparrow P_{MeOH}$	Case 4 $\uparrow P_{DME}$	Case 5 $\uparrow P_{Ethylene}$	Case 6 $\uparrow P_{CO_2}$	Case 7 $\uparrow P_{Tire}$	σ	Source
P_{NG}	Natural gas prices[1]	\$/MMBtu	5.5	14.4	5.5	5.5	2.1	5.5	5.5	3.0	[45]
P_{Elec}	Hourly elec. price	\$/MWh	96.1	96.1	96.1	96.1	50.0	96.1	96.1	22.1	[46]
P_{MeOH}	Methanol price	\$/kg	0.50	0.50	0.70	0.50	0.1	0.50	0.50	0.2	[47]
P_{DME}	DME price	\$/kg	0.8	0.8	0.8	1.0	0.2	0.8	0.8	0.2	[48]
$P_{Ethylene}$	Ethylene price	\$/kg	1.05	1.05	1.05	1.05	3.4	1.05	1.05	0.4	[49]
P_{CO_2}	CO_2 tax rate	\$/tonne	0	0	0	0	0	100	0	-	[3]
P_{Tire}	Tire tipping fees	\$/tonne	0	0	0	0	0	0	100	-	[3]

Table 3: Parameters used for the Cases 1 - 7. [1]Henry Hub Inflation adjusted Natural Gas prices. [3] The prices are assumed. σ denotes standard deviation based on historical data.

4. Results and Discussion

4.1. Cases 1 - 7

The optimal solutions for the decision variables are presented in Table 4 and the capital costs for the different process sections, the corresponding product portfolio as well as economic and environmental performance (quantified by NPV and direct CO_2 emissions respectively) are presented in Table 5. In the product portfolio section, the values in parenthesis denote the energy fraction of the corresponding product calculated using Equation 10, where the energy contents of all products (except electricity) are given by their LHV.

$$\text{Fraction of Product}_{\,i} = \frac{\text{Energy content}_{\,i}}{\text{Total energy content}} \tag{10}$$

In Case 1 (when all prices take on average values), electricity is generated as the only product. The majority ($\sim$61.8%) of the electricity is generated in the gas turbine with the steam turbine (utilizing steam from the HRSG and RSC) providing the other $\sim$38.2%. In Cases 2 - 5, the product that fetches an unusually high price is favored. Electricity is generated in all cases partly in the steam turbine using steam generated in the RSC and partly in the gas turbine after combustion of off-gases. We note that the prices of DME and methanol in Cases 3 and 4 respectively are assumed to be 1 standard deviation above average, thus these two cases occur with a relatively high probability (assuming normal distribution of price). However, the price of natural gas in Case 2 is assumed to be 3 standard deviations above average thus this scenario occurs with a relatively low probability. In Case 5, with the aim of presenting an operating mode that primarily favors the production of olefins, we lowered P_{NG}, P_{Elec}, P_{MeOH} and P_{DME} and substantially increased $P_{Ethylene}$. The olefins prices are assumed to be $\sim$ 6 standard deviations above average thus this scenario has a very low probability of occurring. However, the operating conditions of the MTO section were not optimized in this work, thus using a different process configuration may result in a higher olefins yield and increase profitability.

Case 6 studies the impact of levying a CO_2 tax with all other prices remaining at average values similar to Case 1. We note that the optimal product portfolio changes drastically from producing electricity in Case 1 to primarily producing methanol in Case 6. This is because electricity generation results in substantially higher direct CO_2 emissions after syngas com-

bustion. Furthermore, all these emissions arise in the flue gas stream thus requiring implementation of an expensive DGA-based postcombustion CO_2 capture scheme prior to sequestration. Conversely, when the methanation or methanol synthesis trains are favored, the majority of emissions ($\sim$89.2%) arise in the selexol units prior to product synthesis; diverting this captured CO_2 stream to sequestration is seen to be more economical than implementing postcombustion CCS. Case 7 represents a scenario in which waste tire tipping fees (P_{Tire}) of 100 \$/tonne are levied. All units remain identical to Case 1. However, the annual net profit and NPV is substantially increased providing a similar result as our previous work [3]. Finally, we note that the one train sulfur removal system is implemented when electricity generation is favored (as this is the only option available) while sulfur removal systems B or C are implemented when SNG or MeOH respectively are favored as the need for a separate COS hydrolysis unit is eliminated.

Case	Units	Case 1 Average	Case 2 $\uparrow P_{NG}$	Case 3 $\uparrow P_{MeOH}$	Case 4 $\uparrow P_{DME}$	Case 5 $\uparrow P_{Ethylene}$	Case 6 $\uparrow P_{CO_2}$	Case 7 $\uparrow P_{Tire}$
m_{tire}	kg/s	26.3	26.0	26.1	26.1	26.1	26.1	26.3
R_{OT}		0.837	0.845	0.887	0.887	0.887	0.887	0.837
$S_{OneTrain}$		1	0	0	0	0	0	1
$c_{WGS,SNG}$		0.000	0.789	0.000	0.000	0.000	0.000	0.000
$c_{WGS,MeOH}$		0.000	0.000	0.620	0.620	0.620	0.620	0.000
S_{SNG}		0.0	1.0	0.0	0.0	0.0	0.0	0.0
S_{MeOH}		0.0	0.0	1.0	1.0	1.0	1.0	0.0
S_{GT}		1.0	0.0	0.0	0.0	0.0	0.0	1.0
$S_{Selexol,B}$		0	1	0	0	0	0	0
$S_{Selexol,C}$		0	0	1	1	1	1	0
$S_{MeOH,prod}$		0.0	0.0	1.0	0.0	0.0	1.0	0.0
S_{DME}		0.0	0.0	0.0	1.0	0.0	0.0	0.0
S_{MTO}		0.0	0.0	0.0	0.0	1.0	0.0	0.0
$S_{PostCCS}$		0.0	0.0	0.0	0.0	0.0	0.0	0.0
S_{PreCCS}		0.0	0.0	0.0	0.0	0.0	1.0	0.0

Table 4: Optimal values of the decision variables.

Case		Case 1 Average	Case 2 $\uparrow P_{NG}$	Case 3 $\uparrow P_{MeOH}$	Case 4 $\uparrow P_{DME}$	Case 5 $\uparrow P_{Ethylene}$	Case 6 $\uparrow P_{CO_2}$	Case 7 $\uparrow P_{Tire}$
Total capital costs	M$	932.0	759.4	867.7	951.0	1056.3	874.6	932.0
Gasification [1]	M$	278.7	278.7	278.7	278.7	278.7	278.7	278.7
ASU	M$	164.6	164.6	192.4	192.4	192.4	192.4	164.6
Sulfur removal (One train) [2]	M$	50.9	0.0	0.0	0.0	0.0	0.0	50.9
Methanation train								
WGS 1	M$	0.0	15.2	0.0	0.0	0.0	0.0	0.0
Sulfur removal	M$	0.0	42.3	0.0	0.0	0.0	0.0	0.0
Selexol 1 CO_2 removal	M$	0.0	29.6	0.0	0.0	0.0	0.0	0.0
Methanation and SNG liquefaction	M$	0.0	76.2	0.0	0.0	0.0	0.0	0.0
Methanol train								
WGS 2	M$	0.0	0.0	15.2	15.2	15.2	15.2	0.0
Sulfur removal	M$	0.0	0.0	42.3	42.3	42.3	42.3	0.0
Selexol 2 CO_2 removal	M$	0.0	0.0	31.8	31.8	31.8	31.8	0.0
Methanol synthesis	M$	0.0	0.0	81.2	81.2	81.2	81.2	0.0
DME synthesis	M$	0.0	0.0	0.0	83.3	0.0	0.0	0.0
MTO	M$	0.0	0.0	0.0	0.0	188.6	0.0	0.0
Electricity generation system [3]	M$	337.6	70.9	110.2	110.2	110.2	110.2	337.6
DGA	M$	-	-	-	-	-	-	-
CO_2 compression & sequestration	M$	-	-	-	-	-	6.9	-
Water systems	M$	47.6	29.3	63.2	63.2	63.2	63.2	47.6
Miscellaneous [4]	M$	52.6	52.6	52.6	52.6	52.6	52.6	52.6
Product [5]								
Electricity	MW (%)	456.9 (100%)	14.3 (2.9%)	18.5 (3.8%)	16.8 (3.8%)	45.7 (24.9%)	15.2 (3.1%)	456.9 (100%)
Liquefied SNG	kg/s (%)	-	9.7 (97.1%)	-	-	-	-	-
Methanol	kg/s (%)			22.4 (96.2%)			22.4 (96.9%)	
DME	kg/s (%)	-	-	-	13.8 (96.2%)	-	-	-
Olefins	kg/s (%)	-	-	-	-	3.0 (75.1%)	-	-
Total thermal output	MW	456.9	497.6	491.7	444.8	183.7	488.4	456.9
Thermal efficiency (LHV)	%	51.2	55.7	55.1	49.8	20.6	54.7	51.2
Direct CO_2 emissions	kg/s	72.3	40.4	37.4	37.4	44.7	4.0	72.3
CO_2 sequestered	kg/s	0.0	0.0	0.0	0.0	0.0	33.4	0.0
Annual Net Profit	M$/yr	169.0	153.4	232.0	201.5	140.3	145.3	211.3
Net Present Value (NPV)	M$	432.0	469.7	959.6	657.8	107.5	306.6	747.9
Total wall time (ANTIGONE)	s	7626.6	5383.8	1057.4	1784.7	2462.6	2363.5	5123.0

Table 5: Results of the economic optimization for the 7 cases. [1] Includes Feedstock and slurry prep, EF gasifier and Ash handling. [2] Sulfur removal includes COS hydrolysis, Selexol-based H_2S removal, and Claus process. [3] Includes the Gas Turbine, HRSG, Steam Turbine and Electricity accessory costs. [4] Miscellaneous includes Instrumentation & Control, Site preparation & improvement and Building & Structures. [5] The values in parenthesis denotes the energy fraction of the corresponding product calculated using Equation 10

4.2. Influence of changing Natural Gas and Electricity Prices

Figure 2 presents the optimal design choice and the primary product attained for a range of natural gas and electricity prices at three different methanol price points. The left graph (low methanol price) shows that, at P_{Elec} and P_{NG} lower than $\sim$ 13.6 \$/MMBtu, DME is favored while liquefied SNG is favored at prices above this. In the centre graph (middle methanol price), methanol is produced at P_{NG} values below $\sim$ 13.4 \$/MMBtu with liquefied SNG produced above this price. In the right graph (high methanol price), methanol is favored at all P_{NG} prices. Electricity production is favored at higher P_{Elec} values. A net positive amount of electricity is generated in all designs. Figures 3 and 4 denote the corresponding NPVs and direct CO_2 emissions. The NPV values increase with increasing P_{NG} and P_{Elec} with primary production of liquefied SNG and electricity respectively. Direct CO_2 emissions are also substantially higher when producing electricity and moderately higher for liquefied SNG for reasons discussed in Section 4.1. There appears to be a nonsmooth transition between the different optimal product portfolios with the NPV graph in Figure 3 exhibiting (continuous) disjunctions between corresponding operating modes. None of the grid points we studied resulted in an optimal design for which polygeneration of more than one fuel or chemical occurs.

4.3. Influence of changing Methanol and DME Prices

Figure 5 presents the optimal design choice with varying P_{MeOH} and P_{DME}, while Figures 6 and 7 denote the corresponding NPVs and direct CO_2 emissions. All three graphs remain unchanged with increasing $P_{Ethylene}$ up to 2.5 \$/kg (more than 3 standard deviations above average), thus we conclude that the production of olefins may not be an optimal design choice under the vast majority of scenarios. Direct CO_2 emissions are substantially larger when electricity is generated. There also appears to be a nonsmooth transition between the different product portfolios.

4.4. Influence of CO_2 tax rates

Figures 8, 9, and 10 present the variation of CO_2 sequestered, CO_2 emitted, Net Present Value and mass of products with increasing P_{CO_2} with the rest of the parameters taking on the values of Cases 1, 2 and 3 respectively. At tax rates below 20 \$/tonne, no CO_2 is sequestered implying transportation and sequestration costs exceed the cost of CO_2 taxes. Above this, pre-combustion CCS is implemented. However, implementing post-combustion

CCS is only favored at tax rates higher than 100 $/tonne. The primary product remains unchanged with increasing CO_2 taxes for Cases 2 and 3. However, for Case 1, electricity is no longer favored as the primary product above tax rates of 10 $/tonne. This is because for electricity generation, all CO_2 emissions arise in the flue gas, thus implementing CCS would require building an additional high-throughput DGA-based CO_2 capture process. In order to avoid this expensive unit, the optimal operation mode changes to favor the production of methanol.

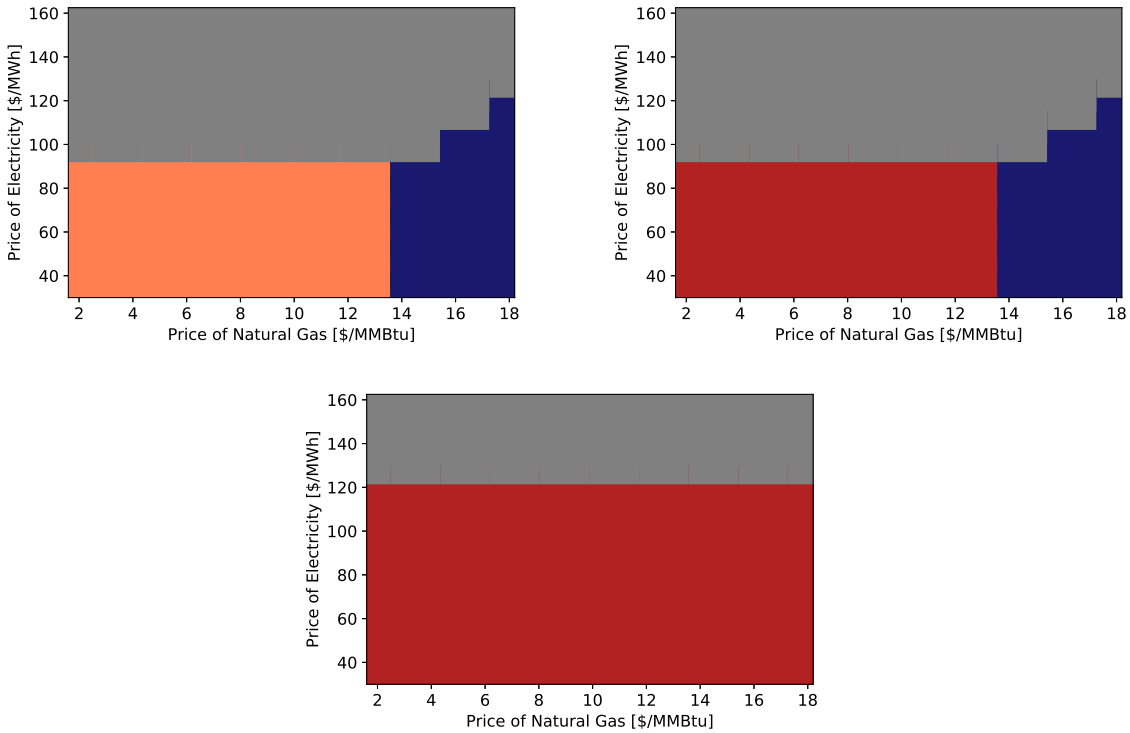

Figure 2: The optimal product choice for a range of natural gas and electricity prices. Three methanol prices are considered: Low (Left), Middle (Centre) and High (Right). All other prices are kept at their averge values. Primary products: : DME, : Electricity, : Methanol, : Liquefied SNG, :Olefins

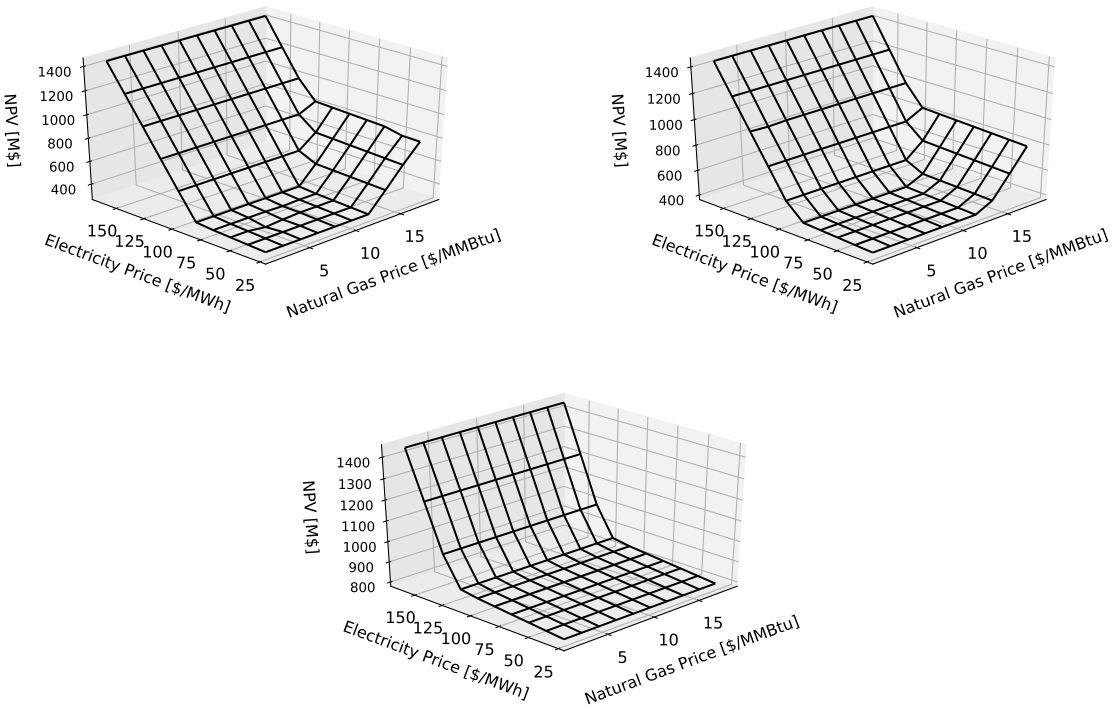

Figure 3: Net Present Values attained for the optimal designs presented in Figure 2

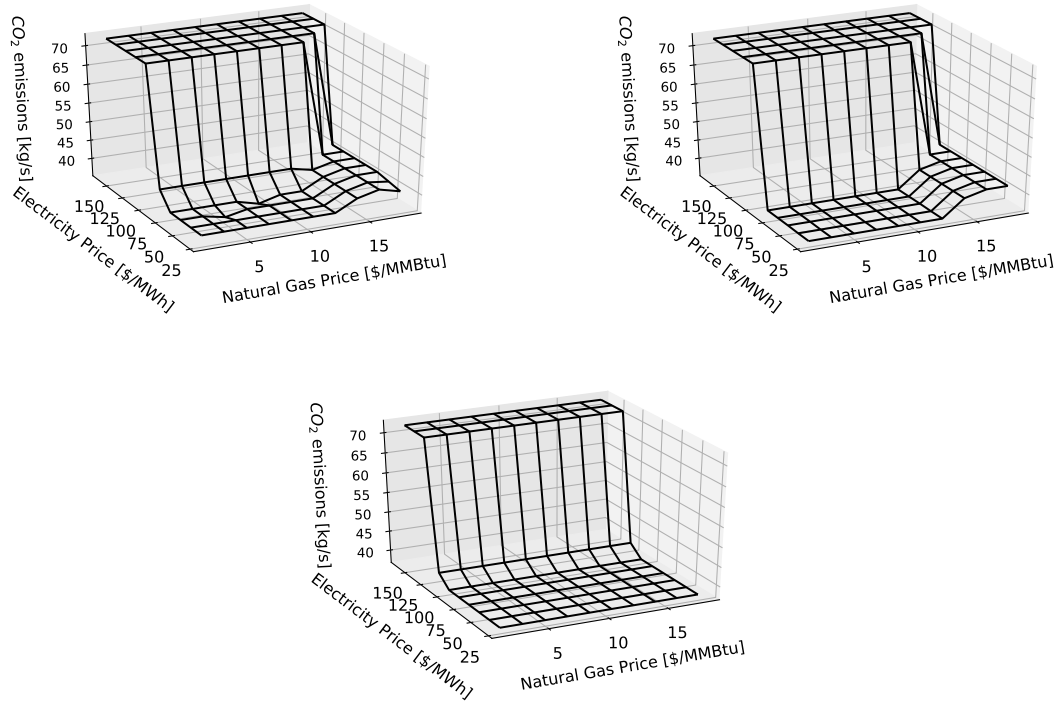

Figure 4: Direct CO_2 emissions for the optimal designs presented in Figure 2

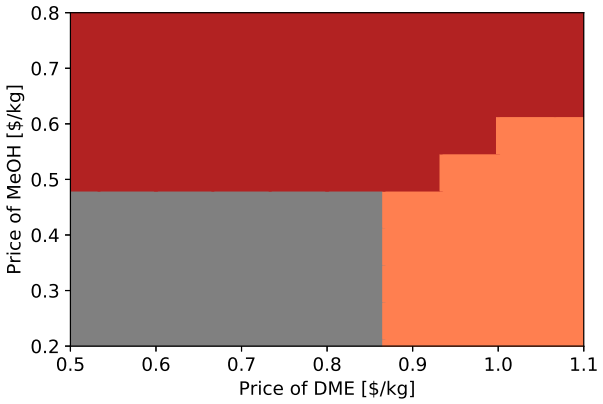

Figure 5: The optimal product choice for a range of MeOH and DME prices. The figure remains unchanged with varying $P_{Ethylene}$ up to 2.5 $/kg. Primary products: : DME, : Electricity, : Methanol, : Liquefied SNG, :Olefins

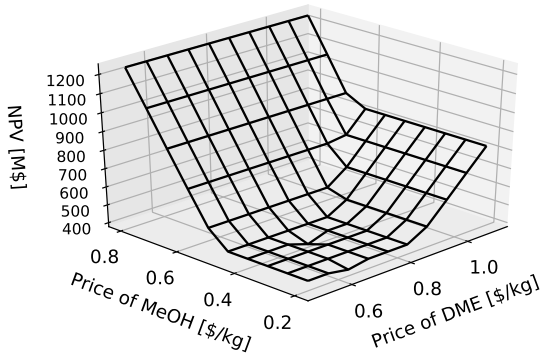

Figure 6: Net Present Values attained for the optimal designs presented in Figure 5.

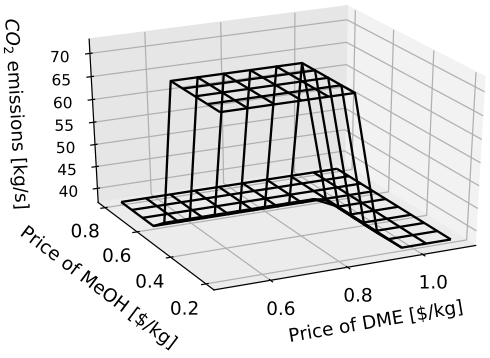

Figure 7: Direct CO_2 emissions for the optimal designs presented in Figure 5

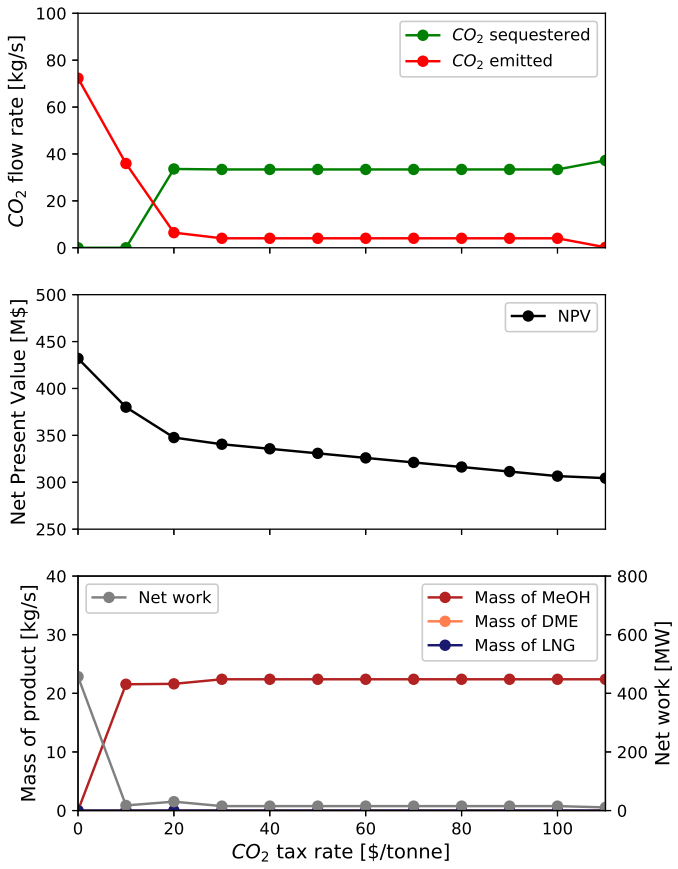

Figure 8: Variation of CO_2 sequestered, CO_2 emitted, Net Present Value and Mass of products with increasing P_{CO_2} for Case 1

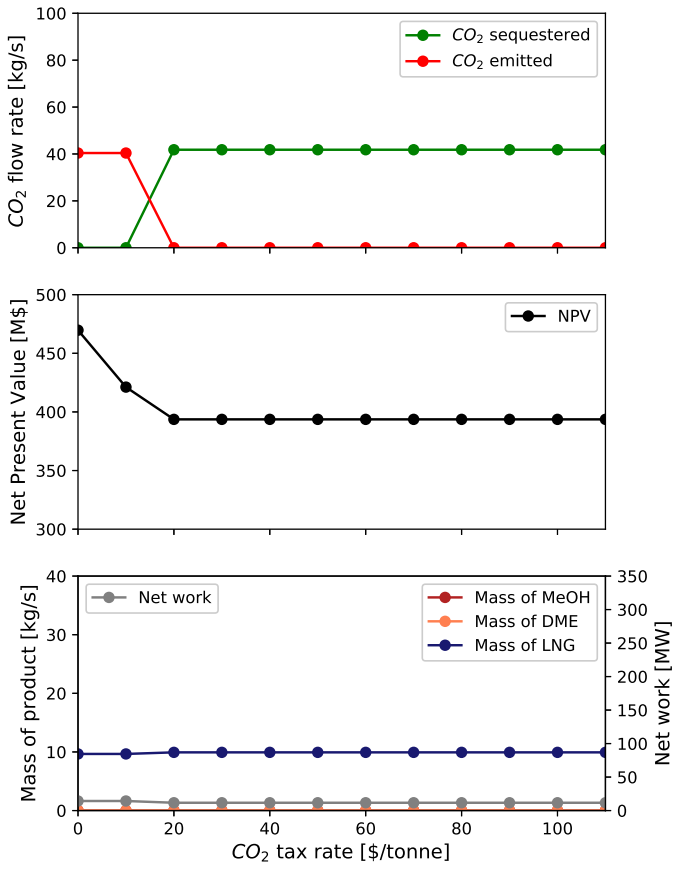

Figure 9: Variation of CO_2 sequestered, CO_2 emitted, Net Present Value and Mass of products with increasing P_{CO_2} for Case 2

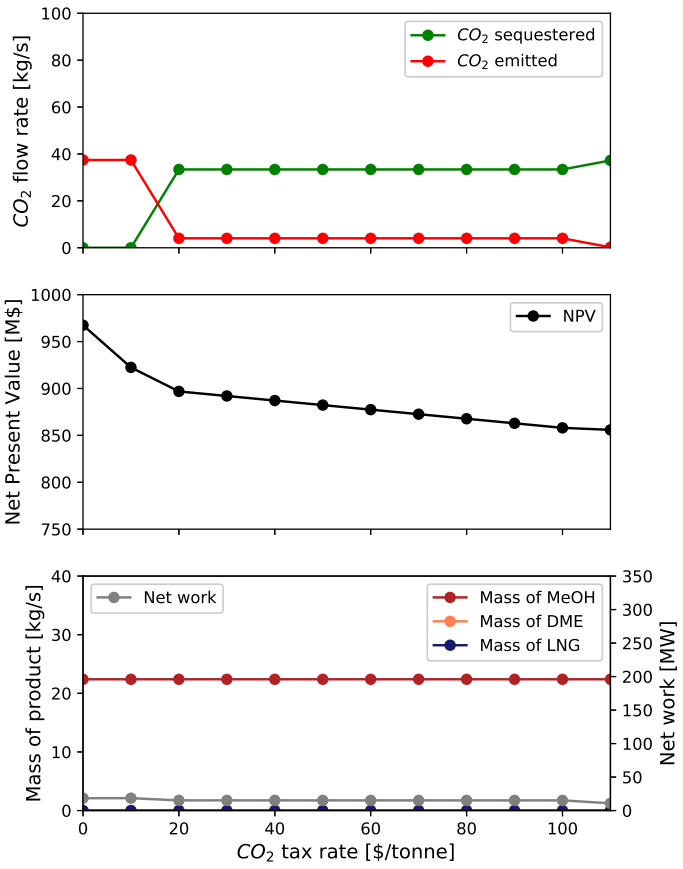

Figure 10: Variation of CO_2 sequestered, CO_2 emitted, Net Present Value and Mass of products with increasing P_{CO_2} for Case 3

5. Conclusions and Future Work

The optimal design and operation of a process converting a waste tire feedstock to potentially several possible products (methanol, liquefied SNG, DME, olefins and electricity) is investigated under a variety of market conditions and CO_2 tax rates. In all scenarios studied, the optimal product portfolio favors generation of one fuel or chemical together with electricity. Electricity generation is favored in a base case with historically average market prices, while methanol, liquefied SNG and DME are favored in relatively probable scenarios in which the corresponding product experiences higher prices. However, the production of olefins is only favored in a scenario that has a low probability of occurrence. Pre-combustion CO_2 capture is favored at lower CO_2 tax rates while post-combustion CO_2 capture is only optimal in scenarios with high CO_2 taxes. Considering that positive NPV values are attained in the historically average base case studied even in the absence of tipping fees, we conclude that the results present an optimistic outlook for the utilization of waste tires in future energy systems.

Considering that the optimal product portfolio changes substantially with varying market conditions, our future work ([50] extended in [51]) will use a stochastic programming approach to investigate the design and operation of a flexible polygeneration process that has the capacity to adjust operating conditions (and modes) in order to maximize profitability by exploiting price peaks.

Acknowledgements

The first author gratefully acknowledges the financial support from NTNU's Department of Energy and Process Engineering and from NTNU Energy. We thank Ikenna J. Okeke, Lingyan Deng and Madison Glover of McMaster University for helpful discussions.

Conflicts of Interest

The authors declare no conflicts of interest.

Nomenclature

$\mathbf{x}$ Operating decision variables

ΔP Pressure change

ΔT_{min} Minimum temperature difference

η_{GT} Efficiency of gas turbine

$\eta_{ST,HQ}$ Efficiency of steam turbine for high quality heat input

$\eta_{ST,LQ}$ Efficiency of steam turbine for low quality heat input

$\nu_{i,r}$ Stoichiometric coefficient of component i in reaction r

$\mathbf{y}$ Design decision variables

ξ_r Extent of reaction r

$c_{WGS,MeOH}$ Overall conversion of CO in the WGS reactors prior to methanol synthesis

$c_{WGS,SNG}$ Overall conversion of CO in the WGS reactors prior to methanation

Cap Total Capital Cost

$f_{in,i}$ Molar flow rates of component i entering a section

$f_{out,i}$ Molar flow rates of component i leaving a section

gr Index for reactions occurring in gasifier

m_{tire} Mass flow rate of waste tire fed to gasifier

N_{rxns} Total number of reactions occuring

Pro_{net} Annual Net Profit

$Q_{GT,in}$ Thermal input to gas turbine

$Q_{HQ,EF}$ Heat duty of the RSC

Q_{HQ_net} High quality heat input to steam turbine system

Q_{LQ_net} Low quality heat input to steam turbine system

r Annual discount rate

R_{OT} Ratio of pure oxygen to tire mass flow rate fed to gasifier

R_{tax} Tax flow rate

S_{DME} Split fraction of methanol product sent to the DME synthesis section

S_{GT} Split fraction of the clean syngas sent to the gas turbine section

$S_{MeOH,prod}$ Split fraction of methanol sold as product

S_{MeOH} Split fraction of the clean syngas sent to the methanol synthesis section

S_{MTO} Split fraction of methanol product sent to MTO synthesis section

$S_{OneTrain}$ Binary choice of one train sulfur removal system

$S_{PostCCS}$ Split fraction of flue gas sent to the DGA-based post-combustion CCS section

S_{PreCCS} Split fraction of CO_2 removed in other plant sections sent to sequestration

$S_{Selexol,B}$ Binary choice of sulfur removal implemented in the methanation train

$S_{Selexol,C}$ Binary choice of sulfur removal implemented in the methanol synthesis train

S_{SNG} Split fraction of clean syngas sent to the methanation section

t_{dp} Depreciation period

t_{lf} Project lifetime

W_{GT} Work of gas turbine

W_{net} Net work

$W_{parastic}$ Parasitic work requirement

W_{ST} Work of steam turbine

CO_2 Carbon dioxide

COS Carbonyl Sulfide

CO Carbon monoxide

H_2O Water

H_2S Hydrogen Sulfide

H_2 Hydrogen

ALAMO Automatic Learning of Algebraic Models for Optimization

ANTIGONE Algorithms for coNTinuous/Integer Global Optimization of Nonlinear Equations

ASU Air Separation Unit

CCS Carbon Capture and Sequestration

DEPG Dimethyl Ether of Polyethylene Glycol

DGA Diglycolamine

DME Dimethyl Ether

EF Entrained Flow (gasifier)

ElecNRTL Electrolyte Non-Random Two-Liquid equation of state

FC Fixed Carbon

GT Gas Turbine

HRSG Heat Recovery Steam Generator

LAPSE Living Archive of Process Systems Engineering

LHV Lower Heating Value

LNG Liquefied Natural Gas

MINLP Mixed-Integer Nonlinear Program

MMBtu Million British thermal units

MSHE Multistream Heat Exchanger

MTO Methanol-To-Olefins process

MW Mega Watts

NLP Nonlinear Program

NPV net Present Value

P Pressure

PR-BM Peng-Robinson equation of state with the Boston-Mathias modification

RKS-VM Redlich-Kwong-Soave equation of state with modified Huron-Vidal mixing rules

RSC Radiant Syngas Cooler

SNG Synthetic Natural Gas

T Temperature

UA_{max}	Maximum heat exchanger conductance	VM	Volatile Matter
		WGS	Water Gas Shift

References

[1] T. A. Adams II, J. H. Ghouse, Polygeneration of fuels and chemicals, Current Opinion in Chemical Engineering 10 (2015) 87–93.

[2] J. D. Martínez, N. Puy, R. Murillo, T. García, M. V. Navarro, A. M. Mastral, Waste tyre pyrolysis: A review, Renewable and Sustainable Energy Reviews 23 (2013) 179–213.

[3] A. S. R. Subramanian, T. Gundersen, T. A. Adams II, Technoeconomic analysis of a waste tire to liquefied synthetic natural gas (SNG) energy system, Energy (2020) 117830.

[4] E. D. Larson, H. Jin, F. E. Celik, Large-scale gasification-based coproduction of fuels and electricity from switchgrass, Biofuels, Bioproducts and Biorefining 3 (2009) 174–194.

[5] Review of Technologies for Gasification of Biomass and Wastes, E4tech. http://www.e4tech.com/reports/review-of-technologies-for-gasification-of-biomass-and-wastes (2009).

[6] H. Boerrigter, A. Van Der Drift, Biosyngas: Description of R&D trajectory necessary to reach large-scale implementation of renewable syngas from biomass, Energy research Centre of the Netherlands (2004).

[7] Y. Chen, T. A. Adams II, P. I. Barton, Optimal design and operation of static energy polygeneration systems, Industrial & Engineering Chemistry Research 50 (2010) 5099–5113.

[8] Y. Chen, T. A. Adams II, P. I. Barton, Optimal design and operation of flexible energy polygeneration systems, Industrial & Engineering Chemistry Research 50 (2011) 4553–4566.

[9] R. C. Baliban, J. A. Elia, C. A. Floudas, Optimization framework for the simultaneous process synthesis, heat and power integration of a thermochemical hybrid biomass, coal, and natural gas facility, Computers & Chemical Engineering 35 (2011) 1647–1690.

[10] R. C. Baliban, J. A. Elia, R. Misener, C. A. Floudas, Global optimization of a MINLP process synthesis model for thermochemical based conversion of hybrid coal, biomass, and natural gas to liquid fuels, Computers & Chemical Engineering 42 (2012) 64–86.

[11] R. C. Baliban, J. A. Elia, C. A. Floudas, Biomass to liquid transportation fuels (BTL) systems: process synthesis and global optimization framework, Energy & Environmental Science 6 (2013) 267–287.

[12] A. M. Niziolek, O. Onel, M. F. Hasan, C. A. Floudas, Municipal solid waste to liquid transportation fuels–part ii: Process synthesis and global optimization strategies, Computers & Chemical Engineering 74 (2015) 184–203.

[13] Y. K. Salkuyeh, T. A. Adams II, Integrated petroleum coke and natural gas polygeneration process with zero carbon emissions, Energy 91 (2015) 479–490.

[14] Y. K. Salkuyeh, A. Elkamel, J. Thé, M. Fowler, Development and techno-economic analysis of an integrated petroleum coke, biomass, and natural gas polygeneration process, Energy 113 (2016) 861–874.

[15] Z. T. Wilson, N. V. Sahinidis, The ALAMO approach to machine learning, Computers & Chemical Engineering 106 (2017) 785–795.

[16] A. Cozad, N. V. Sahinidis, D. C. Miller, Learning surrogate models for simulation-based optimization, AIChE Journal 60 (2014) 2211–2227.

[17] R. Misener, C. A. Floudas, ANTIGONE: Algorithms for Continuous/Integer Global Optimization of Nonlinear Equations, Journal of Global Optimization 59 (2014) 503–526.

[18] I. J. Okeke, T. A. Adams II, Combining petroleum coke and natural gas for efficient liquid fuels production, Energy 163 (2018) 426–442.

[19] J. Klara, M. Woods, P. Capicotto, J. Haslbeck, N. Kuehn, M. Matuszewski, L. Pinkerton, M. Rutkowski, R. Schoff, V. Vaysman, Cost and performance baseline for fossil energy plants volume 1: Bituminous coal and natural gas to electricity. National Energy Technology Laboratory, Research and Development Solutions, LLC (RDS) (2007).

[20] N. Sunthonpagasit, M. R. Duffey, Scrap tires to crumb rubber: feasibility analysis for processing facilities, Resources, Conservation and recycling 40 (2004) 281–299.

[21] M. C. Woods, P. Capicotto, J. L. Haslbeck, N. J. Kuehn, M. Matuszewski, L. L. Pinkerton, M. D. Rutkowski, R. L. Schoff, V. Vaysman, Cost and performance baseline for fossil energy plants, National Energy Technology Laboratory (2007).

[22] C. Kunze, H. Spliethoff, Modelling, comparison and operation experiences of entrained flow gasifier, Energy Conversion and management 52 (2011) 2135–2141.

[23] T. A. Adams II, P. I. Barton, Combining coal gasification and natural gas reforming for efficient polygeneration, Fuel Processing Technology 92 (2011) 639–655.

[24] T. A. Adams II, Y. K. Salkuyeh, J. Nease, Processes and simulations for solvent-based CO2 capture and syngas cleanup, in: Reactor and process design in sustainable energy technology, Elsevier, 2014, pp. 163–231.

[25] R. Brasington, J. Haslbeck, N. Kuehn, E. Lewis, L. Pinkerton, M. Turner, E. Varghese, M. Woods, Cost and Performance Baseline for Fossil Energy Plants — Volume 2: Coal to Synthetic Natural Gas and Ammonia, Technical Report, DOE/NETL-2010/1402, 2011.

[26] N. Kezibri, C. Bouallou, Conceptual design and modelling of an industrial scale power to gas-oxy-combustion power plant, International Journal of Hydrogen Energy 42 (2017) 19411–19419.

[27] H. A. Watson, M. Vikse, T. Gundersen, P. I. Barton, Optimization of single mixed-refrigerant natural gas liquefaction processes described by nondifferentiable models, Energy 150 (2018) 860–876.

[28] Y. Su, L. Lü, W. Shen, et al., An efficient technique for improving methanol yield using dual CO 2 feeds and dry methane reforming, Frontiers of Chemical Science and Engineering (2019) 1–15.

[29] Y. K. Salkuyeh, T. A. Adams II, A new power, methanol, and DME polygeneration process using integrated chemical looping systems, Energy conversion and management 88 (2014) 411–425.

[30] J. A. Scott, T. A. Adams II, Biomass-gas-and-nuclear-to-liquids (BGNTL) processes part I: Model development and simulation, The Canadian Journal of Chemical Engineering 96 (2018) 1853–1871.

[31] Y. Salkuyeh, T. A. Adams II, Co-production of olefins, fuels, and electricity from conventional pipeline gas and shale gas with near-zero CO2 emissions. Part I: process development and technical performance, Energies 8 (2015) 3739–3761.

[32] Y. Chen, Optimal design and operation of energy polygeneration systems, Ph.D. thesis, Massachusetts Institute of Technology, 2013.

[33] H. Er-Rbib, C. Bouallou, Modeling and simulation of CO methanation process for renewable electricity storage, Energy 75 (2014) 81–88.

[34] J. Straus, S. Skogestad, Variable reduction for surrogate modelling, Proceedings of the Foundations of Computer-Aided Process Operations, Tucson, AZ, USA (2017) 8–12.

[35] J. Straus, S. Skogestad, Surrogate model generation using self-optimizing variables, Computers & Chemical Engineering 119 (2018) 143–151.

[36] Living Archive for Process Systems Engineering (LAPSE), `http://psecommunity.org/lapse`, 2019. [Online; accessed 02-August-2019].

[37] R. P. Field, R. Brasington, Baseline flowsheet model for IGCC with carbon capture, Industrial & Engineering Chemistry Research 50 (2011) 11306–11312.

[38] J. Jensen, J. Poulsen, N. Andersen, From coal to clean energy, Nitrogen+ syngas 310 (2011) 34–38.

[39] Z. Y. Yeo, T. L. Chew, P. W. Zhu, A. R. Mohamed, S.-P. Chai, Conventional processes and membrane technology for carbon dioxide removal from natural gas: A review, Journal of Natural Gas Chemistry 21 (2012) 282–298.

[40] K. V. Bussche, G. Froment, A steady-state kinetic model for methanol synthesis and the water gas shift reaction on a commercial Cu/ZnO/Al2O3catalyst, Journal of Catalysis 161 (1996) 1–10.

[41] G. Bercic, J. Levec, Catalytic Dehydration of Methanol to Dimethyl Ether. Kinetic Investigation and Reactor Simulation, Industrial & engineering chemistry research 32 (1993) 2478–2484.

[42] Y. Chen, X. Li, T. A. Adams II, P. I. Barton, Decomposition strategy for the global optimization of flexible energy polygeneration systems, AIChE Journal 58 (2012) 3080–3095.

[43] W. D. Seider, J. D. Seader, D. R. Lewin, Product & Process Design Principles: Synthesis, Analysis and Evaluation, John Wiley & Sons, 2009.

[44] R. Kannan, Algorithms, analysis and software for the global optimization of two-stage stochastic programs, Ph.D. thesis, Massachusetts Institute of Technology, 2017.

[45] U.S. Energy Information Administration. Natural Gas Prices., https://www.eia.gov/dnav/ng/ng_pri_sum_dcu_nus_m.htm, 2020. [Online; accessed 11-June-2020].

[46] Ontario Independent Electricity System Operator (IESO). Hourly Ontario Energy Price, http://www.ieso.ca/en/Power-Data/Price-Overview/Hourly-Ontario-Energy-Price, 2020. [Online; accessed 11-June-2020].

[47] Methanex Monthly Average Regional Posted Contract Price History, https://www.methanex.com/our-business/pricing, 2020. [Online; accessed 11-June-2020].

[48] Alibaba. Dimethyl Ether Prices., https://www.alibaba.com/product-detail/Competitive-dimethyl-ether-prices_60506781674.html?spm=a2700.galleryofferlist.0.0.29d77a22XwD6XM, 2020. [Online; accessed 11-June-2020].

[49] Independent Commodity Intelligence Services. Ethylene US prices., https://www.icis.com/explore/commodities/chemicals/ethylene/us/, 2020. [Online; accessed 11-June-2020].

[50] A. S. R. Subramanian, T. A. Adams II, T. Gundersen, P. I. Barton, Optimal Design and Operation of Flexible Polygeneration Systems using Decomposition Algorithms, in: Computer Aided Chemical Engineering, volume 48, Elsevier, 2020, pp. 919–924.

[51] A. S. R. Subramanian, T. A. Adams II, T. Gundersen, P. I. Barton, Optimal design and operation of a hybrid natural gas and waste tire feedstock flexible polygeneration system using decomposition algorithms, In preparation (2020).